

Effects of temperature and ionic strength on the microscopic structure and dynamics of egg white gels

Cite as: J. Chem. Phys. **158**, 074903 (2023); <https://doi.org/10.1063/5.0130758>

Submitted: 14 October 2022 • Accepted: 26 January 2023 • Accepted Manuscript Online: 30 January 2023 • Published Online: 17 February 2023

 Nafisa Begam,  Sonja Timmermann,  Anastasia Ragulskaya, et al.

COLLECTIONS

Paper published as part of the special topic on [Colloidal Gels](#)



View Online



Export Citation



CrossMark

ARTICLES YOU MAY BE INTERESTED IN

[Rheology of Pseudomonas fluorescens biofilms: From experiments to predictive DPD mesoscopic modeling](#)

The Journal of Chemical Physics **158**, 074902 (2023); <https://doi.org/10.1063/5.0131935>

[Three-step colloidal gelation revealed by time-resolved x-ray photon correlation spectroscopy](#)

The Journal of Chemical Physics **157**, 184901 (2022); <https://doi.org/10.1063/5.0123118>

[Tuning nonequilibrium phase transitions with inertia](#)

The Journal of Chemical Physics **158**, 074904 (2023); <https://doi.org/10.1063/5.0138256>



Time to get excited.
Lock-in Amplifiers – from DC to 8.5 GHz

[Find out more](#)

 Zurich
Instruments

Effects of temperature and ionic strength on the microscopic structure and dynamics of egg white gels

Cite as: J. Chem. Phys. 158, 074903 (2023); doi: 10.1063/5.0130758

Submitted: 14 October 2022 • Accepted: 26 January 2023 •

Published Online: 17 February 2023



View Online



Export Citation



CrossMark

Nafisa Begam,^{1,a)} Sonja Timmermann,² Anastasia Ragulskaya,¹ Anita Girelli,¹
Maximilian D. Senft,¹ Sebastian Retzbach,¹ Nimmi Das Anthuparambil,²
Mohammad Sayed Akhundzadeh,² Marvin Kowalski,² Mario Reiser,³ Fabian Westermeier,⁴
Michael Sprung,⁴ Fajun Zhang,^{1,a)} Christian Gutt,^{2,a)} and Frank Schreiber¹

AFFILIATIONS

¹Institut für Angewandte Physik, Universität Tübingen, 72076 Tübingen, Germany

²Department Physik, Universität Siegen, 57072 Siegen, Germany

³Department of Physics, AlbaNova University Center, Stockholm University, S-106 91 Stockholm, Sweden

⁴Deutsches Elektronen-Synchrotron DESY, Notkestr. 85, 22607 Hamburg, Germany

Note: This paper is part of the JCP Special Topic on Colloidal Gels.

^{a)} **Authors to whom correspondence should be addressed:** nafisa.begam@ifap.uni-tuebingen.de;
fajun.zhang@uni-tuebingen.de; and christian.gutt@uni-siegen.de

ABSTRACT

We investigate the thermal gelation of egg white proteins at different temperatures with varying salt concentrations using x-ray photon correlation spectroscopy in the geometry of ultra-small angle x-ray scattering. Temperature-dependent structural investigation suggests a faster network formation with increasing temperature, and the gel adopts a more compact network, which is inconsistent with the conventional understanding of thermal aggregation. The resulting gel network shows a fractal dimension δ , ranging from 1.5 to 2.2. The values of δ display a non-monotonic behavior with increasing amount of salt. The corresponding dynamics in the q range of 0.002–0.1 nm⁻¹ is observable after major change of the gel structure. The extracted relaxation time exhibits a two-step power law growth in dynamics as a function of waiting time. In the first regime, the dynamics is associated with structural growth, whereas the second regime is associated with the aging of the gel, which is directly linked with its compactness, as quantified by the fractal dimension. The gel dynamics is characterized by a compressed exponential relaxation with a ballistic-type of motion. The addition of salt gradually makes the early stage dynamics faster. Both gelation kinetics and microscopic dynamics show that the activation energy barrier in the system systematically decreases with increasing salt concentration.

Published under an exclusive license by AIP Publishing. <https://doi.org/10.1063/5.0130758>

I. INTRODUCTION

The study of functional properties of proteins is of significance not only in food industry and biotechnology, but also in the areas of soft matter and chemical physics due to their relevance in polymers and colloidal systems.^{1–7} Among various functional properties of proteins, gelation makes them very fascinating scientifically.^{3,8,9} Gelation of proteins involves complex processes, such as coagulation or denaturation, aggregation, and gel network formation.⁴ During thermal gelation, the native proteins unravel, exposing the buried hydrophobic/sulfhydryl groups, and form aggregates via cross-linking.^{9,10} Irreversible aggregates are then formed via covalent

and non-covalent bonds. When the concentration is high enough, the aggregates grow until they occupy the entire space, forming a three-dimensional space-spanning fractal gel network.¹¹ Such a gel exhibits various fascinating properties, e.g., elasticity and water-holding capacity.

To describe the natural aggregation or gelation processes in complex systems, colloidal aggregation processes have been simulated by adapting various interaction potentials.^{12,13} At the microscopic level, the inter-particle interaction primarily tunes the activation energy of the aggregation.¹⁰ Tsai *et al.* investigated the aggregation process of charge-stabilized colloidal particles and revealed that the kinetics is governed by the height of the activation

energy.¹⁴ Gao *et al.* estimated the activation energy of the aggregation related to the critical coagulation concentration that drives the rate of structural growth for a colloidal system.¹⁵ The activation energy is thus crucial in an aggregation process to determine the aggregate structure.^{10,13,14,16} In addition, experiments have shown that the gelation condition influences the aggregate/gel structure substantially.¹¹ For instance, a significant change in the network texture and compactness is recognized in the presence of additives.^{17,18} This structure of the aggregates is mainly responsible for their macroscopic properties.¹⁵ Numerous studies have been carried out to elucidate the structure–function relationship of a gel.^{17,18} Experimental investigation of heat-induced protein gels revealed various fractal structures and their relation to rheological properties.¹¹ However, the phenomenon has appeared to be complex due to non-trivial interactions of the additives with the intrinsic complex charge distribution of proteins, and a systematic understanding of the gel structure influenced by the additives has not been achieved yet.

In addition to the structure, a comprehensive understanding of the protein gel properties requires a systematic investigation of the microscopic dynamics, importantly at the length-scales of the network mesh size. A gel is a non-equilibrium system, which exhibits rich and complex dynamics, especially during aging.¹⁹ For example, various gels are found to be heterogeneous, both in time and space.²⁰ Colloidal gel dynamics displays heterogeneity as a result of large-scale structural deformation during aging.^{19,21} The theory of potential energy landscape describes that, during aging, the system dynamics hops between the local energy minima.^{22,23} In the field of protein gelation, the literature provides information largely on the fast dynamics in a protein gel related to the individual molecular or sub-molecular length-scales.^{24–28} Despite the importance, a complete picture of the microscopic dynamics in a gel at the length-scales related to the network mesh is yet to be established. For a comprehensive understanding of protein-based gels, the structure–dynamics relationship is crucial, as it is generally for any behavior of proteins.²⁹ Our previous investigation on egg white during thermal gelation has contributed to the understanding of the process of thermal aggregation of egg white and the presence of stress driven heterogeneous microscopic dynamics.³⁰

In this work, we investigate egg white to reveal the effect of temperature and salt ions on the structural and dynamical evolution during gel formation using x-ray photon correlation spectroscopy (XPCS) in ultra-small angle x-ray scattering geometry (USAXS). We observe that the structural growth is faster at higher gelation temperatures. We identify two regimes in the dynamics. The early stage dynamics exhibits a rapid growth in the relaxation time, which is determined by the structural evolution. The later-stage dynamics is driven by the gel network compactness. This work also emphasizes the tunability of the activation energy by varying ionic strength in a protein-based system. Our findings provide information on the structure–dynamics relationship in the process of gelation on the length-scales related to the gel network, relevant for fundamental physics, as well as for applications of proteins, polymers, and colloids.

II. SAMPLES AND EXPERIMENTAL DETAILS

We extracted egg white from an organic hen-egg and stored it at 4 °C. Hen-egg white contains more than 40 types of proteins with

an overall concentration of ~110 mg/ml.^{31,32} During thermal denaturation of egg white, native proteins first convert into denatured proteins and then form reversible aggregates via intermolecular β -sheet interactions.³³ The aggregation process⁹ in this system effectively sets in at temperatures above 60 °C. The salt NaCl was used as purchased (Merck, Germany) for the sample preparation. A certain quantity of the salt was directly added to the egg white samples to make the final concentrations ranging from 50 to 150 mM. The final solutions were gently stirred (manually) for ~10 min to dissolve the salt. Thus, the obtained protein solutions were then transferred to quartz capillaries of diameter 1.5 mm to perform x-ray experiments. The capillaries were mounted on a temperature-controlled sample stage. The samples were heated to temperatures above the denaturation temperature of the egg white proteins to produce the gel, and, simultaneously, XPCS measurements^{34–37} were performed. The heating rate used for all the measurements is ~150 °C/min. At this rate, the sample requires ~22 and 30 s to reach temperatures of 75 and 90 °C, respectively. The sample-filled capillary tube is inserted inside the temperature-controlled metal part of the Linkam stage. As a result, the entire part of the capillary that is inside this heating module is expected to be heated to the set temperature.

XPCS in USAXS geometry was employed to probe the structural evolution and dynamics at the length-scales related to the gel network.^{30,38,39} An x-ray beam of size 100 × 100 μm^2 and 8.54 keV photon energy (corresponding to a wavelength $\lambda = 0.145$ nm) was incident on the sample. Time series of the scattering patterns were collected using an Eiger X 4M detector. The experimental setup is schematically illustrated in Fig. S1(a) in the [supplementary material](#). The sample-to-detector distance was 21.2 m to cover a q range from 0.002 to 0.1 nm^{-1} . Several consecutive measurements of a short time period (160 s) were conducted using attenuators to minimize the influence of x rays on the sample (for details, see the [supplementary material](#)).^{40–44} Each of these measurements, performed on a fresh sample spot, consists of 4000 scattering patterns, with 40 ms exposure time. The scattering patterns were then integrated azimuthally to obtain intensity profiles, providing information on the structural evolution during gelation.

The same scattering patterns were correlated over time to extract two-time correlation (TTC) functions for investigating the time-dependent dynamics, which is given by^{40,41,45,46}

$$C_I(q, t_1, t_2) = \frac{\langle I(q, t_1)I(q, t_2) \rangle_{\text{pixels}}}{\langle I(q, t_1) \rangle_{\text{pixels}} \langle I(q, t_2) \rangle_{\text{pixels}}}, \quad (1)$$

where the ensemble average is performed over the pixels within a range $q \pm dq$. Here, q is given by $\frac{4\pi}{\lambda} \sin(\frac{2\theta}{2})$, 2θ being the scattering angle, and the correlation was calculated between the scattering intensities at times t_1 and t_2 . The calculation was done for q from 4.8×10^{-3} to 0.1 nm^{-1} (above which the counting statistics is too weak), with 18 equal $\frac{dq}{q}$ partitions.

III. RESULTS AND DISCUSSION

A. Kinetics of thermal gelation at the sub-micrometer length-scale

Representative USAXS profiles during gelation of the pure egg white samples are shown in Fig. 1(a). An increase in the intensity as a function of waiting time t_w is visible after ~20 s

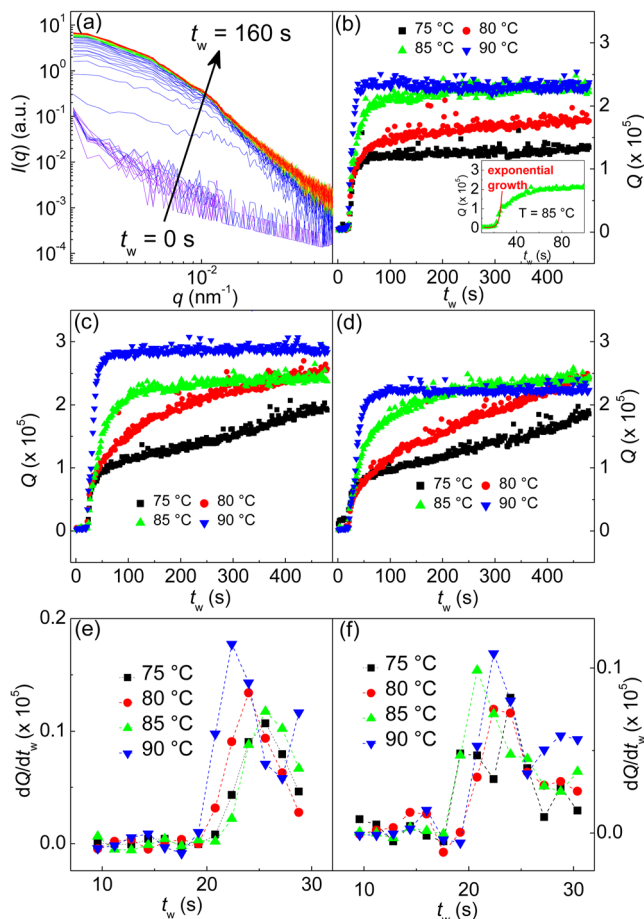


FIG. 1. (a) Intensity profiles $I(q)$ for the pure egg white sample at a temperature of 85 °C at different waiting time t_w ($t_w = 0$ s is when the heating and the measurement started), (b) Q obtained from $I(q)$ as a function of the waiting time for pure egg white, (c) for egg white with 50 mM NaCl, and (d) for egg white with 150 mM NaCl, depicting the development of the gel structure at different temperatures. The time derivative of Q for egg white with (e) 50 mM, and (f) 150 mM NaCl shows the temperature dependence of the structural growth. The inset in panel (b) shows the presence of initial rapid exponential growth in the structure.

of heating. During thermal gelation, the proteins undergo conformational changes via unfolding, and the denatured proteins cross-link to form aggregates. Furthermore, formation of sulfhydryl (SH)/disulfide (SS) bonds within the aggregates establishes the gel.³³ The evolution in the intensity reflects the growth of the fractal aggregates. The growth is initially rapid, then gradually slows down and eventually shows almost no change, depicting no further development in the structure in the observed length-scale window ($q \sim 0.002\text{--}0.05 \text{ nm}^{-1}$). This behavior suggests the process of an initial rapid cross-linking, followed by a gradual establishment of the network at the later stage.^{30,47} To determine the structural growth kinetics, we calculated the invariant from the intensity profiles, which gives a measure of the flocculation parameter, using the relation^{48,49}

$$Q = \int I(q)q^2 dq. \quad (2)$$

The integration is done within the q range of $0.002\text{--}0.03 \text{ nm}^{-1}$ (i.e. the entire q range excluding the background noise). The waiting time-dependence of Q at different temperatures is summarized in Figs. 1(b)–1(d). We observe that the evolution of Q values obtained at different sample spots consistently follow each other (with respect to the range of fluctuations in Q) as a function of measurement time. Therefore, measurements at different spots of the sample were combined to obtain information for longer measurement times. Observation on pure egg white in the early stage [Fig. 1(b)] indicates that Q increases rapidly at all temperatures. The initial rapid structural development for all the samples can be described by an exponential growth function, as illustrated in the inset of Fig. 1(b). Interestingly, Q for the samples with NaCl, especially at lower temperatures, does not attain a constant value [see Figs. 1(c) and 1(d)]. In this case, Q continues to grow even after 400 s of waiting time. In addition, it is important to note that, in all the cases, the speed at which the initial structural change occurs increases with increasing temperature. This behavior can be observed more clearly in Figs. 1(e) and 1(f) in terms of the time derivative of Q . A higher value of the derivative suggests a faster structural change. It is well established that the probability of protein denaturation is enhanced with increasing denaturation temperature.¹⁰ Concomitantly, the probability of aggregation increases as the degree of denaturation increases. The influence of temperature on the gelation kinetics, i.e. the faster structural growth at higher temperatures, is thus associated with the impact of the degree of thermal denaturation. The higher thermal energy at a higher temperature leads to a faster denaturation, and, hence, a faster aggregation.¹⁰

Figures 2(a) and 2(b) show Q as a function of t_w at various salt concentrations, at 80 and 90 °C, respectively. We observe a non-monotonic dependence of the structural evolution on the salt concentration. At all temperatures, at a certain t_w , Q first increases and then decreases as the salt concentration increases. This is visible more clearly at higher temperatures when Q reaches its plateau [depicted in Fig. 1(f)]. The higher Q in the presence of a small amount of salt suggests a larger fraction of proteins participating in the aggregation process compared to that without salt. The presence of salt generally induces a shielding effect on the inter-protein repulsive interactions.⁵⁰ Under these conditions, the aggregation is energetically favored. The higher Q could be associated with such an effect of added salt. As the salt concentration increases, the surface

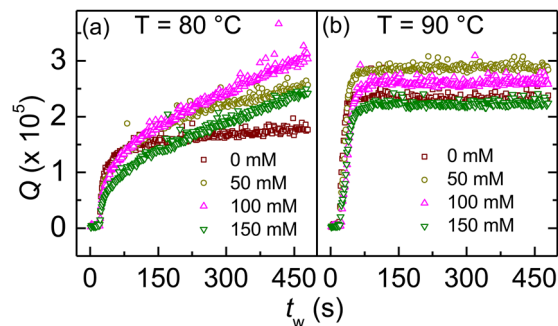


FIG. 2. Salt concentration dependence of Q : the comparison of egg white gelation at various salt concentrations at a temperature of (a) 80 °C, and (b) 90 °C.

charge distribution of the proteins becomes anisotropic.^{2,51} The proteins then form non-ordered cross-links,² compared to the relatively ordered aggregates, in the absence of salt. The aggregation process is spontaneously delayed. An increase in denaturation temperature of egg white proteins has been associated with such non-ordered aggregation processes.² As a result, the system consists of a smaller fraction of denatured proteins compared to that at lower salt concentrations. Consequently, a reduction in Q is observed with increasing salt concentration.

Furthermore, the change in aggregation rate with changing the salt concentration could be related to the change in the activation energy or the height of the energy barrier (ΔE) via the relation $t_c \sim e^{\frac{\Delta E}{RT}}$, where T is the absolute temperature, R is the gas constant, and t_c is the gelation time.^{14,52–55} We have estimated the approximate gelation time t_c from the Q vs t_w plot [see Fig. 3(a)] by considering the point where the major change in Q finishes. At lower temperatures (75 and 80 °C), the point where the extrapolated Q reaches the value of Q at 90 °C is considered as t_c [see Fig. 3(a)]. The estimated t_c values are shown in Fig. 3(b), from which we have determined the activation energy⁵² and shown it in the inset of Fig. 3(b). We observe that ΔE reduces as a function of salt concentration.^{4,10,56} Moreover, ΔE shows an exponential dependence on the salt concentration, as visualized by the dashed line in the inset of Fig. 3(b).

For a quantitative description of the gel structure, the fractal dimension δ was evaluated by modeling⁵⁷ the intensity profiles using the equation $I(q) \sim q^{-\delta}$. The fractal dimension is a quantity that reflects the distribution of intermolecular distances on different length-scales.⁵⁷ δ gives the degree of filling the space by the structure. The fit was performed within the q range 0.0025 to 0.005 nm⁻¹ (i.e., the low q regime) to obtain information on large length-scales relevant for the gel network. The variation of δ as a function of t_w for different gelation processes is presented in Figs. 4(a)–4(d).

Figures 4(a)–4(c) display a fast increase in δ , as the aggregates grow in size during the gelation. Especially at higher temperatures, δ eventually reaches its maximum value when the structural growth is nearly finished. The values of δ for all the samples at all temperatures

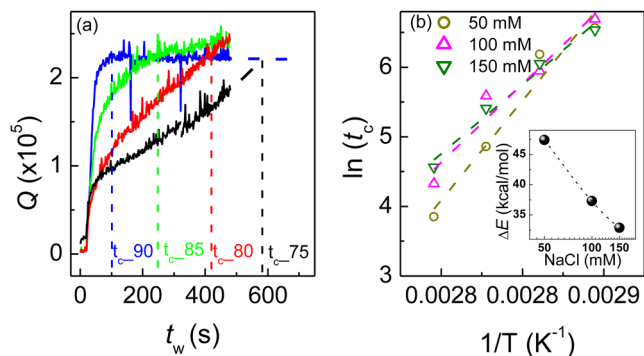


FIG. 3. (a) Estimation of the approximate gelation time t_c from the Q vs t_w behavior is shown by the dashed lines, and (b) $\ln(t_c)$ as a function of $1/T$ is shown for different salt concentrations. The inset depicts the estimated activation energy as a function of salt concentration. A reduction in activation energy is observed with increasing salt concentration.

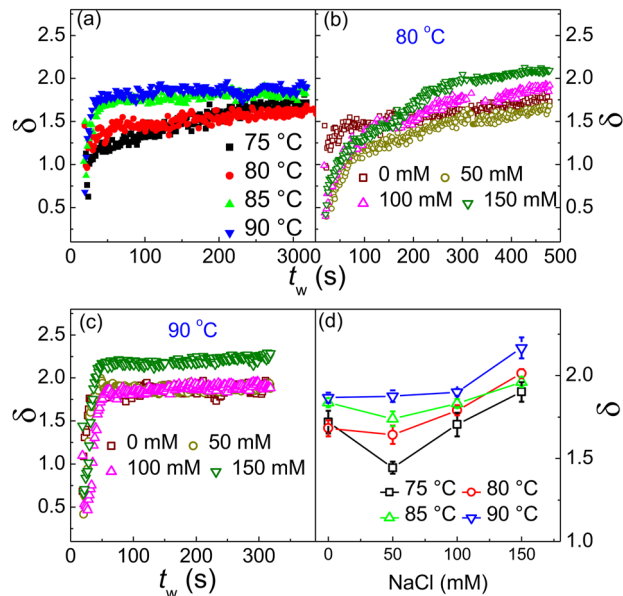


FIG. 4. Fractal dimension δ as a function of t_w for (a) pure egg white at the temperatures indicated by the legends, and for different salt concentrations at (b) 80 °C, (c) 90 °C, and (d) the temperature-dependence of δ for all the samples, as indicated by the legend.

investigated presently range from 1.5 to 2.2, which is interpreted as the strong-link regime in a gelation process where inter-aggregate cross-links are stronger than the cross-links within the aggregates.¹¹ At lower temperatures, δ continues to increase for a longer time, whereas at 90 °C, δ reaches its maximum value as fast as in 50 s of heating. δ for the pure egg white at the temperature of 90 °C is ~ 2 [see Fig. 4(a)], suggesting that the gelation is governed by a reaction-limited aggregation (RLA) process. Interestingly, this value appears to be smaller (< 1.8) at lower temperatures, suggesting a diffusion-limited aggregation (DLA) process. The wide range of δ is possibly due to different aggregation processes involved at different stages of gelation in the system.⁵³

Figures 4(b) and 4(c) depict the propagation of δ in the presence of salt at temperatures of 80 and 90 °C, respectively. The salt-dependence of δ is summarized in Fig. 4(d). Here, δ is averaged over ten data points at the end of the measurements. It is interesting to observe that δ first decreases and then increases as a function of salt concentration. The higher value of δ at a higher salt concentration indicates a more compact gel formation.^{1,58} The less compact gel formation at smaller salt concentrations could be associated with the redistribution of surface charges.⁵¹ The anisotropic interaction between proteins due to anisotropic charge distribution generates a network with lesser branches, i.e. a network with low δ . As the salt concentration increases further, δ starts to increase. The literature suggests that the amount of SH and SS bonds is controlling the gel strength/compactness and hence is responsible for δ .⁵⁰ This observation is consistent with the expectation that a faster aggregation (a higher Q) leads to a smaller δ and vice versa. At a lower salt concentration (at 50 mM), a faster aggregation (higher Q) forms a network with smaller δ , whereas, at higher concentrations

(100–150 mM), a comparatively slower aggregation results in a network with higher δ . The increase in δ with NaCl concentration is consistent with rheological reports showing an increase in the storage modulus of a protein gel with increasing salt amount.⁵¹ An increase in gel compactness generally suggests an increase in the aggregate volume fractions ϕ , which, in turn, is expected to increase Q . This is because Q can be expressed as⁴⁸

$$Q \sim \Delta\rho^2\phi(1-\phi), \quad (3)$$

where $\Delta\rho$ is the electron density contrast. However, currently, we observe that an increase in δ (with increasing salt concentration) is accompanying a reduction in Q . Assuming $\Delta\rho$ does not change significantly during gelation time, we realize that the value of Q can decrease with increasing ϕ only when ϕ is higher than 0.5 in the aggregates. It is possible that as the salt concentration increases, the reduced activation energy causes an increase in ϕ (i.e. decrease in Q , given that $\phi > 0.5$), which subsequently enhances the compactness, as observed in Fig. 4(d). Nevertheless, we do not have any experimental evidence to confirm this statement. This remains still an open question with the need for further investigations.

The kinetics of gelation as a function of temperature (as displayed in Fig. 4) reveals that, overall, δ increases with increasing temperature. In the case of the salt effect, we observed that a slower aggregation leads to a higher δ . However, in the case of temperature dependence, a faster aggregation, as observed at a higher temperature via Q (in Fig. 1), results in a network with a higher δ [in Fig. 4(d)]. This is in contrast to the literature on protein aggregations claiming that normally the temperature effect is likely to reduce the fractal dimension.⁵⁹ On the other hand, rheological studies suggest that the strength of a gel increases with increasing temperature.^{2–4,60} In this respect, the present finding of an increase in compactness with increasing temperature is consistent. The strength is arising from the compactness of the network. The origin could be the extent of inter-aggregate cross-linking.¹¹ At higher temperatures, the probability of inter-aggregate cross-linking increases, which results in a more compact gel network. As a consequence, the observed δ appears to be higher at higher temperatures, whereas at lower temperatures, the gel network is slightly open in nature, due to less inter-aggregate cross-linking.⁶¹

B. Dynamics of egg white gel

In this section, we discuss how the network formation influences the gel dynamics. We calculated TTCs [Eq. (1)] to probe the evolving microscopic dynamics. This calculation produces a correlation map, as presented in Fig. 5, consisting of intensity correlations between time t_1 and t_2 at the waiting time $t_w = (t_1 + t_2)/2$. Hence, the diagonal axis (i.e. $t_1 = t_2$ axis) represents t_w , and the lines perpendicular to this axis are the one-time correlation functions as a function of the elapsed time $t = |t_1 - t_2|$. These cuts are called “constant sample age” cuts.^{62–64} The one-time correlation functions are also often extracted by considering the horizontal or vertical lines, which use the delay time along the rows or columns,⁶³ i.e., lines at constant t_1 or constant t_2 . In the present investigation, the “constant sample age cuts” were considered for further analysis. This method has been widely used to investigate the evolving dynamics during gelation or similar phase transitions in colloidal and various other systems.^{19,62,65} Especially when the system does not experience any

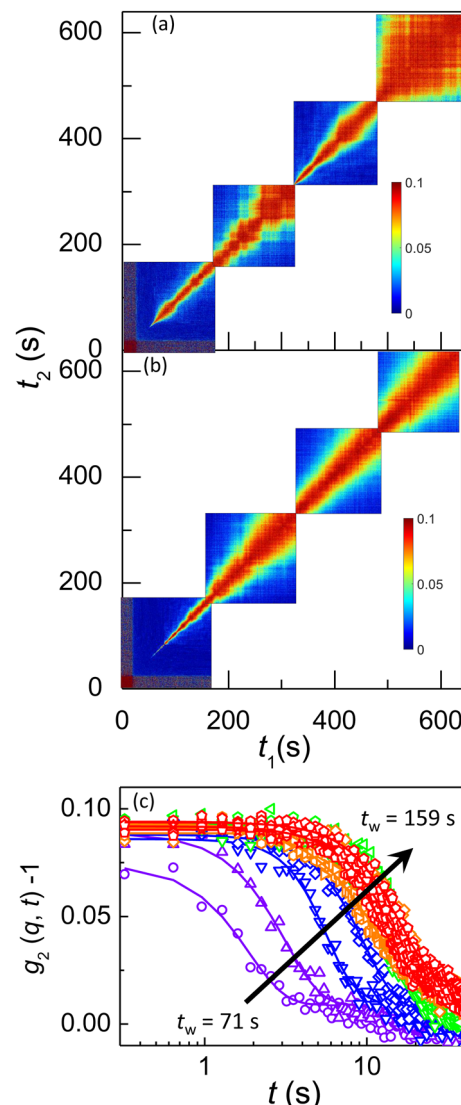


FIG. 5. Representative TTCs collected on (a) pure egg white and (b) egg white at an NaCl concentration of 100 mM during thermal gelation at 80 °C and $q = 0.012 \text{ nm}^{-1}$. (c) line profiles extracted from the first TTC of panel (a), representing g_2 functions as a function of waiting time. Solid lines show fits to the data.

sudden external disturbance, this method has been employed successfully. In this method, the correlations are calculated between intensities before and after the measurement time $(t_1 + t_2)/2$. Therefore, in the case of a sudden external perturbation in the system, the mixing of the time before and after $(t_1 + t_2)/2$ could lead to a non-reliable interpretation. However, in the present case, there is no such scenario, and, thus, the method is suitable for the system.

The calculation of TTCs is performed using the MATLAB code XPCSGUI provided by the P10 beamline (Petra III, DESY, Germany). TTCs calculated for the pure egg white sample and that in the presence of salt of concentration 100 mM are shown in Figs. 5(a)

and 5(b), respectively. The width of the diagonal contour (along the $t_1 = t_2$ axis) of the TTC map is proportional to the characteristic time-scale of the system. We observe from the TTCs that the dynamics exhibits a considerable slowdown with t_w for both samples.⁶⁶ Note that each of these TTCs is collected on a fresh spot on the capillaries. As we can see in Fig. 5(a), the dynamics grows in the first TTC, followed quite consistently by a similar growth rate of the second TTC. However, the third TTC does not seem to be consistent with the previous TTCs, possibly because this spot differs in its thermal history, which is not surprising as such a complex protein system like egg white can show spatial variations in the concentrations of different proteins.

In Fig. 5, the dynamics is observable only after a certain measurement time (60–70 s) in the probed length-scale window ($q \sim 0.002\text{--}0.05\text{ nm}^{-1}$). Comparing that with the structural evolution [in Figs. 1(b)–1(d)], we could see that the system time-scale appears in the experimental window approximately after the major structural growth is finished. Line profiles were extracted from these TTCs and averaged over 4 s to obtain the one-time correlation functions $g_2(q, t)$ at different t_w . The correlation functions for a pure egg white sample at $q = 0.012\text{ nm}^{-1}$ are representatively shown in Fig. 5(c). These correlation functions can be described by^{45,64,65}

$$g_2(q, t) = 1 + \beta |g_1(q, t)|^2, \quad (4)$$

with a Kohlrausch–Williams–Watts (KWW) function^{45,64}

$$g_1(q, t) = \exp[-(t/\tau)^\gamma], \quad (5)$$

where β is the instrumental scattering contrast, τ is the characteristic relaxation time, and γ is the KWW exponent, describing the nature of the dynamics. In this model, the exponent γ is 1 for diffusive dynamics, exhibiting a purely exponential relaxation decay. Systems that are arrested, e.g., glasses, often have been observed to show $\gamma < 1$, which corresponds to a stretched exponential relaxation decay.^{67,68} On the other hand, $\gamma > 1$ is observed in systems characterized by hyper-diffusive dynamics.^{30,38,39,64}

1. Temperature dependence

The obtained $g_2(q, t)$ functions were modeled using Eq. (4), and the time evolution of τ for different salt concentrations and temperatures are shown in Fig. 6. In the initial stage, τ grows rapidly, and then the growth slows down, indicating aging of the gel.^{65,69} In this regime, for most of the samples, τ exhibits fluctuations with time (see Fig. 6). The literature suggests that the internal stresses in the gel network produced during cross-linking result in the aging dynamics.¹⁹ Relaxation of these stresses gives rise to large-scale rearrangements. The fluctuations in τ have been attributed to such structural rearrangements that occur on a large length-scale in the gel network.^{19,30} Note that a two-step evolution of τ is present in most of the cases. However, at 75 °C, only the later-stage dynamics, and at 90 °C (e.g., for the pure egg white sample), possibly the early stage dynamics are probed. This could be due to experimental limitations (i.e. the limited time window from milliseconds to the total measurement time). Nevertheless, it is interesting to observe that a more rapid growth in τ is apparent with increasing temperature. Consequently, in the second regime, τ reaches a higher value (via more rapid growth in τ) at a higher temperature. In other words, the dynamics is slower at a higher temperature (see Fig. 6) and faster at

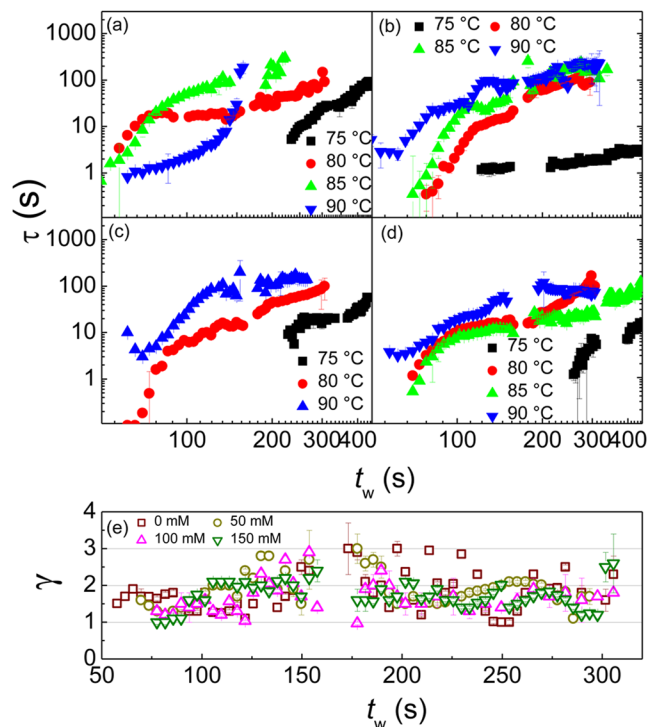


FIG. 6. Temperature-dependent relaxation time τ obtained by modeling g_2 functions at $q = 0.012\text{ nm}^{-1}$ for (a) pure egg white; (b) egg white with 50 mM, (c) 100 mM, and (d) 150 mM NaCl, and (e) representative plot of γ as a function of waiting time for samples with different salt concentrations at 80 °C.

a lower temperature. We note here that Chuskin *et al.* have reported an inversely proportional dependence of the de-correlation time on photon flux.⁴⁶ Therefore, for long measurement times, a contribution of the beam-induced de-correlation in the measured dynamics may still be possible, even at low photon flux. Nevertheless, the evidence of the second regime in dynamics is robust, as in most of the samples, the second regime appears at small t_w (see Fig. S4 in the supplementary material).

The process of denaturation, structural evolution of the aggregates, and their dependence on the temperature is determined by the activation energy barrier of the system.¹⁰ At a higher temperature, the denaturation and, thus, the aggregation process is thermodynamically more favorable, as it is easier to exceed the energy barrier, which corresponds to faster gelation kinetics.¹⁰ The initial rapid growth in τ is possibly influenced directly by the gelation kinetics. A faster kinetics of gelation at a higher temperature leads to a faster increase in τ . Note that the evolution in the dynamics does not occur simultaneously with the structural evolution. The rapid network formation generates the trapped-stresses, and the dynamics is accompanying the relaxation of these stresses. As a result, the growth in dynamics is following the structural growth. After the formation of the network structure, we observed a more compact gel network formation (see δ in Fig. 4) at a higher temperature. Concomitant with the compactness, Fig. 6 displays a slower dynamics

at a higher temperature. This observation is consistent with the concept of a thermal gel. Our results provide evidence that the dynamics of a thermal gel is determined by the interplay between the thermal energy and the compactness of the gel network, and the influence of the compactness is considerably strong to completely overtake the thermal energy-driven dynamics.

The KWW exponent γ is observed to fluctuate around 2 for all the samples, depicting a compressed exponential relaxation dynamics in the system, as representatively shown in Fig. 6(e). Such a unique compressed exponential decay suggests a hyper-diffusive dynamics, which has been observed in a stress-driven gel dynamics.^{30,70} The structural rearrangements to release the internal stresses result in the intermittent hyper-diffusive dynamics. This contradicts the thermal energy-driven diffusive processes, where a simple exponential decay ($\gamma = 1$) is observed.⁷¹

To quantify the temperature-dependence of the dynamics, we plotted τ rescaled by a factor, ν . Here, ν is determined by dividing τ at all temperatures by the τ of the pure egg white at 75 °C in the overlapping time range and then averaging them. Those data (e.g., egg white at 90 °C) having no overlap regime (in t_w) with the dataset of pure egg white at 75 °C were excluded from this analysis. We can see in Fig. 7(a) that the rescaled τ for all samples falls on a master curve, in particular, in the second regime. This observation of τ falling onto a master curve supports the existence of the two distinct regimes (as shown by the green and white background) in the dynamics as a function of t_w in all the cases. Note that, in most of the samples, the transition between the two regimes in the

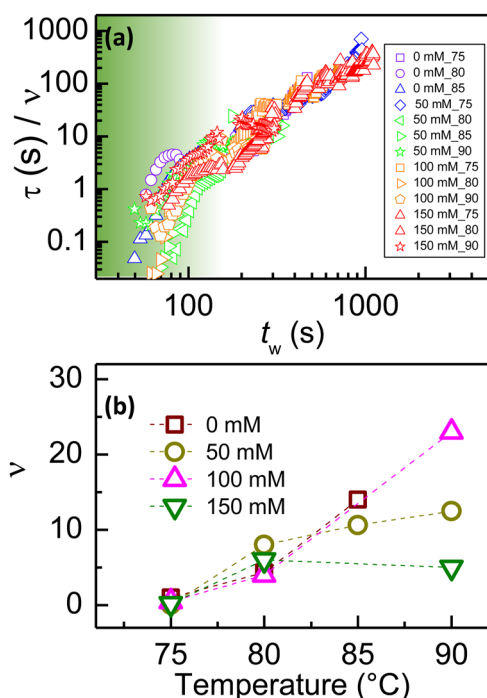


FIG. 7. (a) Rescaled τ at different temperatures for all the samples at $q = 0.012 \text{ nm}^{-1}$ and (b) the obtained values of ν as a function of temperature. The two distinct regimes are indicated by the background color in (a).

dynamics is observable within the first 160 s of measurement time (see Fig. S4 in the [supplementary material](#)). This behavior supports the presence of a two-step growth in dynamics, irrespective of the spatial heterogeneity in the sample, as observed for TTCs collected at different spots of the sample. The factor ν , shown in Fig. 7(b), overall increases with increasing temperature. The functional dependence of ν on the temperature emphasizes the scaling of the rate of change in τ with temperature. We note here that ν does not show the same temperature dependence for all the salt concentrations. At salt concentrations below 100 mM, ν monotonically increases with temperature. However, at 150 mM salt concentration [green triangle in Fig. 7(b)], the behavior appears to be different. Such a complex temperature dependence of the dynamics could arise from the complex and multi-component protein contents of the egg white. It is important to mention here that the temperature dependence of τ and the presence of two stages in the dynamics with compressed exponential relaxation are observed irrespective of variations between different egg samples. Although the absolute values of the relaxation time may change, the overall nature of the dynamics remains unaltered.

2. Salt concentration dependence

The salt dependence of τ at temperatures 80 and 90 °C is shown in Fig. 8. Notably, the two-step growth in dynamics appears to be a function of the salt concentration. The initial growth in τ (green background) becomes less steep with increasing salt. However, at a later stage, τ is higher (white background) for higher salt concentrations. To assess the effect of salt on the gel dynamics, we have modeled τ vs t_w with two power law equations, i.e. $\tau \sim t_w^n$. From the fit, we obtained the exponents, n , that define the growth rate. The exponent shown in Fig. 8(c), in the early stage, exhibits very high value, suggesting an exponential behavior, as observed previously.³⁰ The exponent, in this regime, overall decreases with NaCl and at the later stage, increases or remains constant with increasing NaCl. The early stage growth is determined by the structural evolution, where we observed that the salt concentration initially enhances (for 50 mM) and then reduces (for 100 and 150 mM) the structural evolution. In τ , though we do not observe a clear enhancement in the growth rate at 50 mM salt, the growth becomes shallower with further increasing salt, consistent with the structural kinetics. Nevertheless, the later-stage dynamics (aging) seems to follow the compactness and stiffness of the gel. This is a further confirmation of the finding that the dynamics during aging is dictated by the gel compactness. For clarity, we have used background color in Figs. 8(a) and 8(b) to distinguish the two dynamical regimes. The first regime (green background) is where the growth in τ is mainly accompanied by structural growth. The second regime (white background) is driven by the compactness of the gel.

We further note that the gel compactness is sensitive to the system dynamics in the early stage. The faster dynamics in the presence of salt, in the early stage, suggests the higher probability of restructuring events in the gel. Now, we recall the observation of the increase in δ with increasing salt as shown in Fig. 4(d). Existing reports⁷² on protein gelation have claimed that the restructuring of aggregates can cause such an increase in δ . The increase in δ , here, manifests the effect of restructuring on the gel compactness.

The q dependence of τ is shown in Fig. 9(a) for the pure egg white samples. As we can see, τ weakly depends on q , and it varies

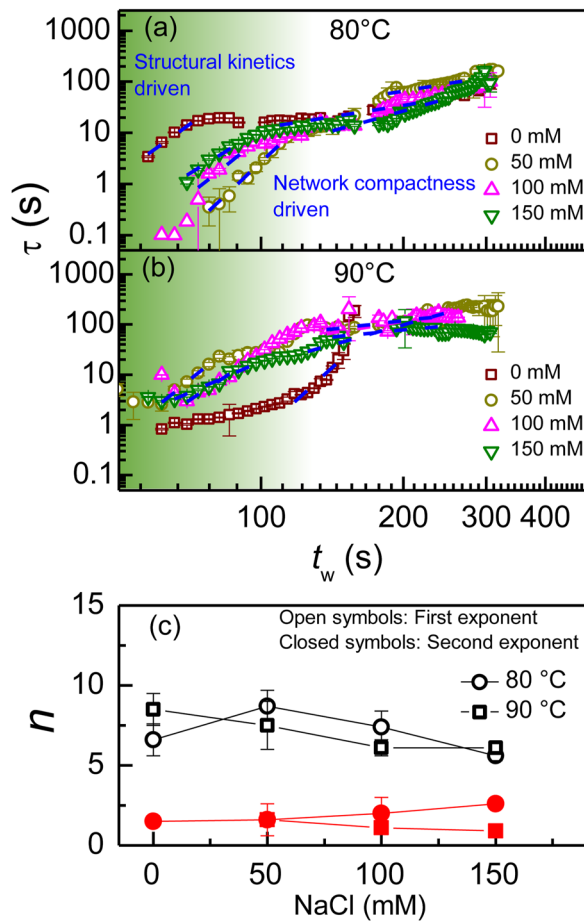


FIG. 8. (a) τ as a function of t_w at different salt concentrations at 80 °C (a) and 90 °C (b) showing two-step power law growth at $q = 0.012 \text{ nm}^{-1}$. (c) The early stage exponent (open symbols), and the later-stage exponent (closed symbols) of the power-law functions at 80 °C (circles) and 90 °C (squares) are revealing the effect of salt on the aggregation energy barrier, respectively. The dashed lines in (a) and (b) indicate the power law fits.

slightly with t_w . We modeled the q dependence of τ with a power law relation $\tau \sim q^{-\alpha}$ and obtained α , as presented in Figs. 9(b)–9(d). Here, α appears to be fluctuating around 1. This is in contrast to the case of diffusive dynamics,⁷³ where α is 2. The observation of $\alpha \sim 1$ and $\gamma \sim 2$ [see Fig. 6(e)] indicates ballistic dynamics.^{30,73} Moreover, in some cases, e.g., the pure egg white sample at the temperature of 90 °C, the fluctuation is large, as α varies from 0.5 to 1.6. We speculate that the fluctuation arises from the discrete large-scale rearrangements, to reduce the degree of stresses in the network. The observation of a weak power law dependence of τ on q has been linked with the internal stress driven dynamics.^{19,65} The currently observed temporal fluctuation in τ [see Figs. 6(a)–6(d)] is consistent with this length-scale dependence, indicating the structural rearrangements during aging.^{30,35} However, the coupling between the growth and the temporal fluctuations of τ , as can be seen in the TTCs [Fig. 5(a)], makes it difficult to quantify the dynamical heterogeneity that arises from the reorganization events. Therefore, focusing only

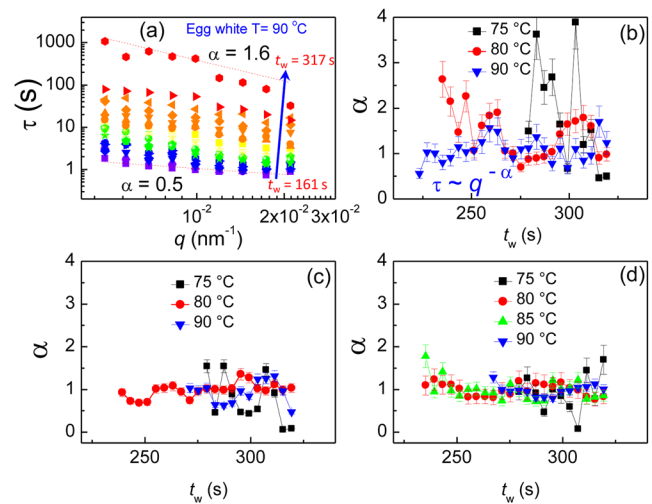


FIG. 9. (a) τ as a function of q at different t_w for the pure egg white sample at 90 °C, showing the length-scale dependence, and the exponent α as a function of time for (b) pure egg white, (c) with a salt concentration of 100 mM, and (d) 150 mM at different temperatures, as shown by the legends.

on the length-scale dependence, we observe that at the temperature of 75 °C for the pure egg white sample, α tends to exhibit a higher value, as is expected for a diffusive Brownian system. Slower evolution of structure at a lower temperature is likely to produce a smaller degree of stress in the network. As a result, the effect of internal stress on the dynamics could be weaker in the gels that are produced at lower temperatures. The dynamics then could behave differently. However, due to the noisy data, the length-scale dependence is not conclusive at lower temperatures.

IV. CONCLUSIONS

In conclusion, our investigation on egg white proteins during gelation at various temperatures shows changes in the growth of structure, associated with thermal energy-driven protein denaturation, followed by an aggregation process. The gel network compactness increases with increasing temperature. The influence of salt on the gelation kinetics, and the result provide the scaling of the activation energy as a function of salt concentration. The presence of salt initially enhances and then reduces the speed at which the network forms. The rapid growth of the fractal structure accompanies the growth in the relaxation dynamics. The effect of higher thermal energy at a higher temperature is suppressed by the slower dynamics driven by the gel compactness. As a result, the relaxation time increases with increasing temperature. We identify two distinct regimes of dynamics, where the first regime is linked with the structural development and the second regime is determined by the gel compactness and the structural rearrangements. The presence of salt leads to a faster dynamics in the early stage and a slower or no change in the dynamics at the later stage. The gel dynamics shows a compressed exponential decay and an inversely proportional length-scale dependence of the relaxation time. Such a scenario suggests a ballistic-type motion in the system, arising from the release of internal stresses via structural rearrangements.

SUPPLEMENTARY MATERIAL

See the [supplementary material](#) for the discussion of the beam influence on the structure and dynamics of egg white via USAXS and TTC data analysis.

ACKNOWLEDGMENTS

We gratefully acknowledge the support of DFG and BMBF for this work. The authors would also like to thank the DESY (Hamburg, Germany), a member of the Helmholtz Association, HGF, for the provision of experimental facilities. Parts of this research were carried out at the PETRA III beamline P10. C.G. acknowledges the BMBF (BMBF 05K19PS1, 05K20PSA, and 05K22PS1), A.R. acknowledges the Studienstiftung des deutschen Volkes, and N.B. acknowledges the Alexander von Humboldt Foundation.

AUTHOR DECLARATIONS

Conflict of Interest

The authors have no conflicts to disclose.

Author Contributions

Nafisa Begam: Conceptualization (lead); Data curation (lead); Formal analysis (lead); Investigation (equal); Visualization (lead); Writing – original draft (lead); Writing – review & editing (lead). **Sonja Timmermann:** Investigation (supporting); Visualization (supporting); Writing – review & editing (supporting). **Anastasia Ragulskaya:** Investigation (lead); Writing – review & editing (supporting). **Anita Girelli:** Visualization (supporting); Writing – review & editing (supporting). **Maximilian D. Senft:** Investigation (supporting); Writing – review & editing (supporting). **Sebastian Retzbach:** Investigation (supporting); Writing – review & editing (supporting). **Nimmi Das A:** Writing – review & editing (supporting). **Mohammad Sayed Akhundzadeh:** Investigation (supporting). **Marvin Kowalski:** Investigation (supporting). **Mario Reiser:** Software (supporting). **Fabian Westermeier:** Methodology (equal); Software (supporting); Writing – review & editing (supporting). **Michael Sprung:** Methodology (equal); Software (supporting). **Fajun Zhang:** Conceptualization (equal); Project administration (equal); Supervision (equal); Visualization (equal); Writing – review & editing (equal). **Christian Gutt:** Project administration (equal); Visualization (equal); Writing – review & editing (equal). **Frank Schreiber:** Project administration (lead); Visualization (supporting); Writing – review & editing (equal).

DATA AVAILABILITY

The data that support the findings of this study are available within the article.

REFERENCES

¹C. Schmitt, C. Moitz, C. Bovay, M. Rouvet, L. Bovetto, L. Donato, M. E. Leser, P. Schurtenberger, and A. Stradner, “Internal structure and colloidal behaviour of covalent whey protein microgels obtained by heat treatment,” *Soft Matter* **6**, 4876–4884 (2010).

²V. Raikos, L. Campbell, and S. R. Euston, “Rheology and texture of hen’s egg protein heat-set gels as affected by pH and the addition of sugar and/or salt,” *Food Hydrocolloids* **21**, 237–244 (2007).

³A. Handa, K. Takahashi, N. Kuroda, and G. W. Froning, “Heat-induced egg white gels as affected by pH,” *J. Food Sci.* **63**, 403–407 (1998).

⁴J. Li, Y. Zhang, Q. Fan, C. Teng, W. Xie, Y. Shi, Y. Su, and Y. Yang, “Combination effects of NaOH and NaCl on the rheology and gel characteristics of hen egg white proteins,” *Food Chem.* **250**, 1–6 (2018).

⁵N. Zhao, N. L. Francis, H. R. Calvelli, and P. V. Moghe, “Microglia-targeting nanotherapeutics for neurodegenerative diseases,” *APL Bioeng.* **4**, 030902 (2020).

⁶G. F. Paciotti, L. Myer, D. Weinreich, D. Goia, N. Pavel, R. E. McLaughlin, and L. Tamarkin, “Colloidal gold: A novel nanoparticle vector for tumor directed drug delivery,” *Drug Delivery* **11**, 169–183 (2004).

⁷J. E. Straub and D. Thirumalai, “Toward a molecular theory of early and late events in monomer to amyloid fibril formation,” *Annu. Rev. Phys. Chem.* **62**, 437–463 (2011).

⁸Y. Mine, T. Noutomi, and N. Haga, “Thermally induced changes in egg white proteins,” *J. Agric. Food Chem.* **38**, 2122–2125 (1990).

⁹K. Iwashita, N. Inoue, A. Handa, and K. Shiraki, “Thermal aggregation of hen egg white proteins in the presence of salts,” *Protein J.* **34**, 212–219 (2015).

¹⁰J. C. Bischof and X. He, “Thermal stability of proteins,” *Ann. N. Y. Acad. Sci.* **1066**, 12–33 (2006).

¹¹M. M. Ould Eleya, S. Ko, and S. Gunasekaran, “Scaling and fractal analysis of viscoelastic properties of heat-induced protein gels,” *Food Hydrocolloids* **18**, 315–323 (2004).

¹²E. Zaccarelli, P. J. Lu, F. Ciulla, D. A. Weitz, and F. Sciortino, “Gelation as arrested phase separation in short-ranged attractive colloid–polymer mixtures,” *J. Phys.: Condens. Matter* **20**, 494242 (2008).

¹³D. Spagnoli, J. F. Banfield, and S. C. Parker, “Free energy change of aggregation of nanoparticles,” *J. Phys. Chem. C* **112**, 14731–14736 (2008).

¹⁴D.-H. Tsai, L. F. Pease III, R. A. Zangmeister, M. J. Tarlov, and M. R. Zachariah, “Aggregation kinetics of colloidal particles measured by gas-phase differential mobility analysis,” *Langmuir* **25**, 140–146 (2009).

¹⁵X. Gao, Q. Kou, K. Ren, Y. Zuo, Y. Xu, Y. Zhang, R. Lal, and J. Wang, “Quantitative characterization of non-DLVO factors in the aggregation of black soil colloids,” *Sci. Rep.* **12**, 5064 (2022).

¹⁶S. Lu, Y. Ding, and J. Guo, “Kinetics of fine particle aggregation in turbulence,” *Adv. Colloid Interface Sci.* **78**, 197–235 (1998).

¹⁷E. Martin, M. Prostredny, A. Fletcher, and P. Mulheran, “Modelling organic gel growth in three dimensions: Textural and fractal properties of resorcinol–formaldehyde gels,” *Gels* **6**, 23 (2020).

¹⁸L. Campbell, V. Raikos, and S. R. Euston, “Modification of functional properties of egg-white proteins,” *Food/Nahrung* **47**, 369–376 (2003).

¹⁹A. Fluerasu, A. Moussaïd, A. Madsen, and A. Schofield, “Slow dynamics and aging in colloidal gels studied by X-ray photon correlation spectroscopy,” *Phys. Rev. E* **76**, 010401 (2007).

²⁰E. Lattuada, D. Caprara, R. Piazza, and F. Sciortino, “Spatially uniform dynamics in equilibrium colloidal gels,” *Sci. Adv.* **7**, eabk2360 (2021).

²¹N. Şenbil, M. Gruber, C. Zhang, M. Fuchs, and F. Scheffold, “Observation of strongly heterogeneous dynamics at the depinning transition in a colloidal glass,” *Phys. Rev. Lett.* **122**, 108002 (2019).

²²B. Doliwa and A. Heuer, “What does the potential energy landscape tell us about the dynamics of supercooled liquids and glasses?,” *Phys. Rev. Lett.* **91**, 235501 (2003).

²³A. Heuer, “Exploring the potential energy landscape of glass-forming systems: From inherent structures via metabasins to macroscopic transport,” *J. Phys.: Condens. Matter* **20**, 373101 (2008).

²⁴M. Hennig, F. Roosen-Runge, F. Zhang, S. Zorn, M. W. A. Skoda, R. M. J. Jacobs, T. Seydel, and F. Schreiber, “Dynamics of highly concentrated protein solutions around the denaturing transition,” *Soft Matter* **8**, 1628–1633 (2012).

²⁵O. Matsarskaia, L. Bühl, C. Beck, M. Grimaldo, R. Schweins, F. Zhang, T. Seydel, F. Schreiber, and F. Roosen-Runge, “Evolution of the structure and dynamics of bovine serum albumin induced by thermal denaturation,” *Phys. Chem. Chem. Phys.* **22**, 18507–18517 (2020).

- ²⁶T. Nagano, H. Mori, and K. Nishinari, "Effect of heating and cooling on the gelation kinetics of 7S globulin from soybeans," *J. Agric. Food Chem.* **42**, 1415–1419 (1994).
- ²⁷F. Massi, J. W. Peng, J. P. Lee, and J. E. Straub, "Simulation study of the structure and dynamics of the alzheimer's amyloid peptide congener in solution," *Biophys. J.* **80**, 31–44 (2001).
- ²⁸M. Moron, A. Al-Masoodi, C. Lovato, M. Reiser, L. Randolph, G. Surmeier, J. Bolle, F. Westermeier, M. Sprung, R. Winter *et al.*, "Gelation dynamics upon pressure-induced liquid–liquid phase separation in a water–lysozyme solution," *J. Phys. Chem. B* **126**, 4160–4167 (2022).
- ²⁹M. Grimaldo, F. Roosen-Runge, F. Zhang, F. Schreiber, and T. Seydel, "Dynamics of proteins in solution," *Q. Rev. Biophys.* **52**, E7 (2019).
- ³⁰N. Begam, A. Ragulskaia, A. Girelli, H. Rahmann, S. Chandran, F. Westermeier, M. Reiser, M. Sprung, F. Zhang, C. Gutt, and F. Schreiber, "Kinetics of network formation and heterogeneous dynamics of an egg white gel revealed by coherent X-ray scattering," *Phys. Rev. Lett.* **126**, 098001 (2021).
- ³¹N. Koshoubu, H. Kanaya, K. Hara, S. Taki, E. Takushi, and K. Matsushige, "Variations of mechanical properties in egg white during gel-to-glasslike transition," *Jpn. J. Appl. Phys.* **32**, 4038 (1993).
- ³²E. D. N. S. Abeyrathne, H. Y. Lee, and D. U. Ahn, "Egg white proteins and their potential use in food processing or as nutraceutical and pharmaceutical agents review," *Poult. Sci.* **92**, 3292–3299 (2013).
- ³³T. Croguennec, F. Nau, and G. Brule, "Influence of pH and salts on egg white gelation," *J. Food Sci.* **67**, 608–614 (2002).
- ³⁴G. Grübel and F. Zontone, "Correlation spectroscopy with coherent X-rays," *J. Alloys Compd.* **362**, 3–11 (2004).
- ³⁵R. L. Leheny, M. C. Rogers, K. Chen, S. Narayanan, and J. L. Harden, "Rheo-XPCS," *Curr. Opin. Colloid Interface Sci.* **20**, 261–271 (2015).
- ³⁶J. Möller, M. Reiser, J. Hallmann, U. Boesenberg, A. Zozulya, H. Rahmann, A.-L. Becker, F. Westermeier, T. Zinn, M. Sprung *et al.*, "Using low dose x-ray speckle visibility spectroscopy to study dynamics of soft matter samples," *New J. Phys.* **23**, 093041 (2021).
- ³⁷J. Möller, M. Sprung, A. Madsen, and C. Gutt, "X-ray photon correlation spectroscopy of protein dynamics at nearly diffraction-limited storage rings," *IUCr* **6**, 794–803 (2019).
- ³⁸A. Girelli, H. Rahmann, N. Begam, A. Ragulskaia, M. Reiser, S. Chandran, F. Westermeier, M. Sprung, F. Zhang, C. Gutt, and F. Schreiber, "Microscopic dynamics of liquid–liquid phase separation and domain coarsening in a protein solution revealed by X-ray photon correlation spectroscopy," *Phys. Rev. Lett.* **126**, 138004 (2021).
- ³⁹A. Ragulskaia, N. Begam, A. Girelli, H. Rahmann, M. Reiser, F. Westermeier, M. Sprung, F. Zhang, C. Gutt, and F. Schreiber, "Interplay between kinetics and dynamics of liquid–liquid phase separation in a protein solution revealed by coherent X-ray spectroscopy," *J. Phys. Chem. Lett.* **12**, 7085–7090 (2021).
- ⁴⁰M. Reiser, A. Girelli, A. Ragulskaia, S. Das, S. Berkowicz, M. Bin, M. Ladd-Parada, M. Filianina, H.-F. Poggemann, N. Begam *et al.*, "Resolving molecular diffusion and aggregation of antibody proteins with megahertz x-ray free-electron laser pulses," *Nat. Commun.* **13**, 5528 (2022).
- ⁴¹J. Song, Q. Zhang, F. de Quesada, M. H. Rizvi, J. B. Tracy, J. Ilavsky, S. Narayanan, E. Del Gado, R. L. Leheny, N. Holten-Andersen, and G. H. McKinley, "Microscopic dynamics underlying the stress relaxation of arrested soft materials," *Proc. Natl. Acad. Sci. U. S. A.* **119**, e2201566119 (2022).
- ⁴²P. Vodnala, N. Karunaratne, S. Bera, L. Lurio, G. M. Thurston, N. Karonis, J. Winans, A. Sandy, S. Narayanan, L. Yasui *et al.*, "Radiation damage limits to XPCS studies of protein dynamics," *AIP Conf. Proc.* **1741**, 050026 (2016).
- ⁴³L. B. Lurio, G. M. Thurston, Q. Zhang, S. Narayanan, and E. M. Dufresne, "Use of continuous sample translation to reduce radiation damage for XPCS studies of protein diffusion," *J. Synchrotron Radiat.* **28**, 490–498 (2021).
- ⁴⁴S. Kuwamoto, S. Akiyama, and T. Fujisawa, "Radiation damage to a protein solution, detected by synchrotron x-ray small-angle scattering: Dose-related considerations and suppression by cryoprotectants," *J. Synchrotron Radiat.* **11**, 462–468 (2004).
- ⁴⁵S. K. Sinha, Z. Jiang, and L. B. Lurio, "X-ray photon correlation spectroscopy studies of surfaces and thin films," *Adv. Mater.* **26**, 7764–7785 (2014).
- ⁴⁶Y. Chushkin, A. Gulotta, F. Roosen-Runge, A. Pal, A. Stradner, and P. Schurtenberger, "Probing cage relaxation in concentrated protein solutions by x-ray photon correlation spectroscopy," *Phys. Rev. Lett.* **129**, 238001 (2022).
- ⁴⁷A. Halabi, A. Deglaire, P. Hamon, S. Bouhallab, D. Dupont, and T. Croguennec, "Kinetics of heat-induced denaturation of proteins in model infant milk formulas as a function of whey protein composition," *Food Chem.* **302**, 125296 (2020).
- ⁴⁸S. Da Vela, N. Begam, D. Dyachok, R. S. Schäufele, O. Matsarskaia, M. K. Braun, A. Girelli, A. Ragulskaia, A. Mariani, F. Zhang, and F. Schreiber, "Interplay between glass formation and liquid–liquid phase separation revealed by the scattering invariant," *J. Phys. Chem. Lett.* **11**, 7273–7278 (2020).
- ⁴⁹F. Zhang, D. G. Dressen, M. W. A. Skoda, R. M. J. Jacobs, S. Zorn, R. A. Martin, C. M. Martin, G. F. Clark, and F. Schreiber, "Gold nanoparticles decorated with oligo (ethylene glycol) thiols: Kinetics of colloid aggregation driven by depletion forces," *Eur. Biophys. J.* **37**, 551–561 (2008).
- ⁵⁰S. Hayakawa and R. Nakamura, "Optimization approaches to thermally induced egg white lysozyme gel," *Agric. Biol. Chem.* **50**, 2039–2046 (1986).
- ⁵¹S. Ikeda, E. A. Foegeeding, and T. Hagiwara, "Rheological study on the fractal nature of the protein gel structure," *Langmuir* **15**, 8584–8589 (1999).
- ⁵²M. A. Da Silva and E. P. G. Arêas, "Solvent-induced lysozyme gels: Rheology, fractal analysis, and sol–gel kinetics," *J. Colloid Interface Sci.* **289**, 394–401 (2005).
- ⁵³D. A. Weitz, J. S. Huang, M. Y. Lin, and J. Sung, "Limits of the fractal dimension for irreversible kinetic aggregation of gold colloids," *Phys. Rev. Lett.* **54**, 1416 (1985).
- ⁵⁴W. Li, B. A. Persson, M. Morin, M. A. Behrens, M. Lund, and M. Zackrisson Oskolkova, "Charge-induced patchy attractions between proteins," *J. Phys. Chem. B* **119**, 503–508 (2015).
- ⁵⁵Q. Li, Y. Tang, X. He, and H. Li, "Approach to theoretical estimation of the activation energy of particle aggregation taking ionic nonclassical polarization into account," *AIP Adv.* **5**, 107218 (2015).
- ⁵⁶Y. Yang, A. J. Welch, and H. G. Rylander III, "Rate process parameters of albumen," *Lasers Surg. Med.* **11**, 188–190 (1991).
- ⁵⁷D. Johansen, J. Trehwella, and D. P. Goldenberg, "Fractal dimension of an intrinsically disordered protein: Small-angle X-ray scattering and computational study of the bacteriophage λ N protein," *Protein Sci.* **20**, 1955–1970 (2011).
- ⁵⁸S. Jungblut, J.-O. Joswig, and A. Eychmüller, "Diffusion-and reaction-limited cluster aggregation revisited," *Phys. Chem. Chem. Phys.* **21**, 5723–5729 (2019).
- ⁵⁹R. Vreeker, L. L. Hoekstra, D. C. Den Boer, and W. G. M. Agterof, "Fractal aggregation of whey proteins," *Food Hydrocolloids* **6**, 423–435 (1992).
- ⁶⁰P. W. Gossett, S. S. H. Rizvi, and R. C. Baker, "A new method to quantitate the coagulation process," *J. Food Sci.* **48**, 1400–1404 (1983).
- ⁶¹Z. Meng, S. M. Hashmi, and M. Elimelech, "Aggregation rate and fractal dimension of fullerene nanoparticles via simultaneous multiangle static and dynamic light scattering measurement," *J. Colloid Interface Sci.* **392**, 27–33 (2013).
- ⁶²G. Brown, P. A. Rikvold, M. Sutton, and M. Grant, "Speckle from phase-ordering systems," *Phys. Rev. E* **56**, 6601 (1997).
- ⁶³O. Bikondoa, "On the use of two-time correlation functions for X-ray photon correlation spectroscopy data analysis," *J. Appl. Crystallogr.* **50**, 357–368 (2017).
- ⁶⁴A. Madsen, R. L. Leheny, H. Guo, M. Sprung, and O. Czakkal, "Beyond simple exponential correlation functions and equilibrium dynamics in X-ray photon correlation spectroscopy," *New J. Phys.* **12**, 055001 (2010).
- ⁶⁵Z. Evenson, B. Ruta, S. Hechler, M. Stolpe, E. Pineda, I. Gallino, and R. Busch, "X-ray photon correlation spectroscopy reveals intermittent aging dynamics in a metallic glass," *Phys. Rev. Lett.* **115**, 175701 (2015).
- ⁶⁶E. Del Gado, A. Fierro, L. de Arcangelis, and A. Coniglio, "Slow dynamics in gelation phenomena: From chemical gels to colloidal glasses," *Phys. Rev. E* **69**, 051103 (2004).
- ⁶⁷D. Orsi, B. Ruta, Y. Chushkin, A. Pucci, G. Ruggeri, G. Baldi, T. Rimoldi, and L. Cristofolini, "Controlling the dynamics of a bidimensional gel above and below its percolation transition," *Phys. Rev. E* **89**, 042308 (2014).
- ⁶⁸A. Nogales and A. Fluerasu, "X ray photon correlation spectroscopy for the study of polymer dynamics," *Eur. Polym. J.* **81**, 494–504 (2016).

⁶⁹B. Chung, S. Ramakrishnan, R. Bandyopadhyay, D. Liang, C. F. Zukoski, J. L. Harden, and R. L. Leheny, “Microscopic dynamics of recovery in sheared depletion gels,” *Phys. Rev. Lett.* **96**, 228301 (2006).

⁷⁰R. Hernández, A. Nogales, M. Sprung, C. Mijangos, and T. A. Ezquerra, “Slow dynamics of nanocomposite polymer aerogels as revealed by X-ray photocorrelation spectroscopy (XPCS),” *J. Chem. Phys.* **140**, 024909 (2014).

⁷¹A. Meyer, “Self-diffusion in liquid copper as seen by quasielastic neutron scattering,” *Phys. Rev. B* **81**, 012102 (2010).

⁷²P. Meakin, “Fractal aggregates,” *Adv. Colloid Interface Sci.* **28**, 249–331 (1987).

⁷³A. Pal, T. Zinn, M. A. Kamal, T. Narayanan, and P. Schurtenberger, “Anomalous dynamics of magnetic anisotropic colloids studied by XPCS,” *Small* **14**, 1802233 (2018).